Journal of Solid State Chemistry **168,** 202–207 (2002)
doi:10.1006/jssc.2002.9710

Structural and Magnetic Chemistry of $La_2Sr_2BMnO_8$ (*B*=Mg, Zn)

Jonathan C. Burley,* Peter D. Battle,*,[1] Peter J. Gaskell,* and Matthew J. Rosseinsky†,[1]

*Inorganic Chemistry Laboratory, Oxford University, South Parks Road, Oxford OX1 3QR, United Kingdom; and †Department of Chemistry, University of Liverpool, Liverpool, L69 7ZD, United Kingdom

Received March 20, 2002; in revised form May 10, 2002; accepted May 15, 2002

Polycrystalline samples of the layered perovskites $La_2Sr_2MgMnO_8$ and $La_2Sr_2ZnMnO_8$ have been studied by X-ray and neutron powder diffraction, electron diffraction and magnetometry. X-ray and neutron powder diffraction indicate that the average structure is that of K_2NiF_4, with disordering of Mn and (Zn, Mg) cations over the octahedral sites. Electron diffraction data indicate that cation ordering is present over these sites in the *xy* planes, with the *xy* ordered planes being stacked in a disordered manner along *z*. No long-range magnetic ordering is observed in the temperature range $5 \leq T$ (K) ≤ 300. © 2002 Elsevier Science (USA)

Key Words: **paracrystals; K_2NiF_4.**

1. INTRODUCTION

In a previous paper (1), we reported the structures of La_4LiMnO_8 and $La_3SrLiMnO_8$, which were shown to possess structures related to that of K_2NiF_4 (2). The Li and Mn cations were shown to be completely ordered within the *xy* sheets of corner-sharing LiO_6–MnO_6 octahedra, with these sheets being stacked in a disordered manner in the *z* direction. This contrasts with the expected *Ammm* crystallographic model (Fig. 1), in which the ordering occurs along all three crystallographic axes. Many of the concepts traditionally associated with crystallography were shown to be inapplicable, and the phases were best described within the paracrystal formalism (3, 4), The main Mn–Mn superexchange was shown to occur through a single *d* orbital (*xy*), and $La_3SrLiMnO_8$ was shown to be an example of a quadratic layer Heisenberg system. The purpose of the present work is to extend the previous study, and to determine whether the features uncovered therein are general to mixed systems which are polytypes of the K_2NiF_4 structure. A number of these polytypes have been investigated in the past (5–13). The cations now chosen for investigation are Mn along with either Zn or Mg. This choice was made as Zn and Mg are expected to be electronically inactive, and thus place the same restriction on Mn–Mn exchange coupling routes as was the case for the La/Sr/Li/Mn/O systems. Both compounds have been prepared previously, and were reported to adopt an unusual structure in space group *P*422, with *xy* Mn:(Zn, Mg) ordered layers interleaved with *xy* disordered layers (14).

2. EXPERIMENTAL

Both $La_2Sr_2MnMgO_8$ and $La_2Sr_2MnZnO_8$ were synthesized using standard ceramic methods. The starting materials, La_2O_3 (99.999%, Alfa), $SrCO_3$ (99.994%, Alfa), MnO_2 (99.999%, Alfa), ZnO (99.99%, Johnson–Matthey) and MgO (99.9955%, Alfa) were used as received, apart from La_2O_3 which was dried at 800°C prior to use. The heating sequence employed for both samples was as follows: 800°C, 24 h, 1200°C, 48 h (O_2), 1350°C, 48 h, (O_2), 1350°C, 48 h (air).

X-ray powder diffraction data suitable for Rietveld analysis were collected on a Siemens D5000 diffractometer scanning in Bragg-Brentano geometry over the angular range $10 \leq 2\theta$ (°) ≤ 120, $\lambda = 1.54059$ Å, $\Delta 2\theta = 0.02°$. Neutron powder diffraction experiments were performed at room temperature on the time-of-flight instruments HRPD and GEM, both at ISIS, Rutherford–Appleton Laboratories. Rietveld analyses (15, 16) were performed using the GSAS program suite (17). In the case of $La_2Sr_2ZnMnO_6$ data collected on three of the GEM detector banks were analyzed simultaneously, whereas in the case of $La_2Sr_2MgMnO_6$ only data collected on the back-scattering detector bank of HRPD were analyzed. Both samples were also studied by electron diffraction. Selected area electron diffraction (SAED) patterns were obtained by use of a double-tilting goniometer stage ($\pm$ 30°) to tilt the specimen in a JEOL 2000 FX transmission electron microscope. The finely ground powders were suspended in hexane and placed on lacey carbon-coated copper grids. Magnetometry

[1] To whom correspondence should be addressed. Fax: +44-1865-2726-90. E-mail: peter.battle@chem.ox.ac.uk, m.j.rosseinsky@liverpool.ac.uk.

0022-4596/02 $35.00

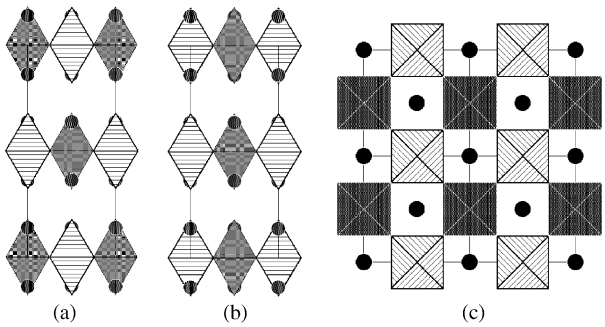

FIG. 1. Idealized views of *Ammm* *B*-site ordered K_2NiF_4 structure type; (a) [100], (b) [010] and (c) [001] projections for 1:1 ordering are shown.

experiments were performed on a Quantum Design MPMS SQUID DC magnetometer, measuring both after cooling in zero field and after cooling in the applied measuring field of 100 Oe.

3. RESULTS

3.1. X-Ray and Neutron Powder Diffraction

The X-ray powder diffraction data for $La_2Sr_2BMnO_8$ (B = Zn, Mg) could be indexed on the basis of an unexpanded tetragonal K_2NiF_4-like unit cell. Rietveld refinements of the data proceeded satisfactorily, and converged swiftly to stable, chemically reasonable minima ($La_2Sr_2MnMgO_8$: $\chi^2 = 1.205$, $R_{wp} = 8.84\%$, $R_p = 6.96\%$; $La_2Sr_2MnZnO_8$: $\chi^2 = 2.184$, $R_{wp} = 12.70\%$, $R_p = 9.69\%$). Refinement of $La_2Sr_2MnZnO_8$ required the incorporation of a small amount of $La(OH)_3$ into the model as a second phase. This phase is diamagnetic and is not expected to affect the interpretation of magnetometry data. The change in oxidation state of Mn as a result of the slight non-stoichiometry of the main phase is also likely to be small enough to be negligible.

Results of a Rietveld analysis of neutron powder diffraction data collected on GEM for $La_2Sr_2ZnMnO_8$ are shown in Fig. 2a, with a K_2NiF_4-like starting model used. The scattering lengths of Mn and Zn are −3.73(2) and 5.680(5) fm, respectively (18), and thus any cation ordering on the six-coordinate site over the length scale probed by a neutron powder diffraction experiment should be visible. It can be seen (Fig. 2a) that an excellent fit of the data is obtained by using a model which contains no cation ordering (overall goodness-of-fit indicators for three histogram refinement: $\chi^2 = 2.222$, $R_{wp} = 3.98\%$, $R_p = 4.35\%$). The structural parameters derived from this refinement are given in Table 1. A small contribution to the diffraction pattern from the presence of a $La(OH)_3$ impurity phase was again included in the model. It can be seen in Table 1 that the Zn/Mn–O_6 octahedra are elongated along the fourfold axis. This is a common feature of the chemistry of K_2NiF_4-like structures, and is a result of the greater ease of relieving chemical pressure in this direction. The atomic displacement parameter for the octahedrally coordinated Mn/Zn site is anomalously large; this reflects the relative insensitivity of neutron powder diffraction to that site, which is occupied in a disordered manner by cations with scattering lengths of opposite signs. Refinements using the orthorhombic *Ammm* space group, which allows for cation ordering, did not lead to an improvement in fit. Comparison of simulated patterns indicated that the refinement would have been sensitive to cation ordering at the 45:55 level.

Neutron powder diffraction data for $La_2Sr_2MgMnO_8$ collected on HRPD at room temperature are shown in Fig. 2b, along with the results of a Rietveld analysis ($\chi^2 = 1.192$, $R_{wp} = 9.01\%$, $R_p = 7.49\%$). The scattering lengths of Mn and Mg are −3.73(2) and 5.375(4) fm, respectively (18), and thus any cation ordering on the

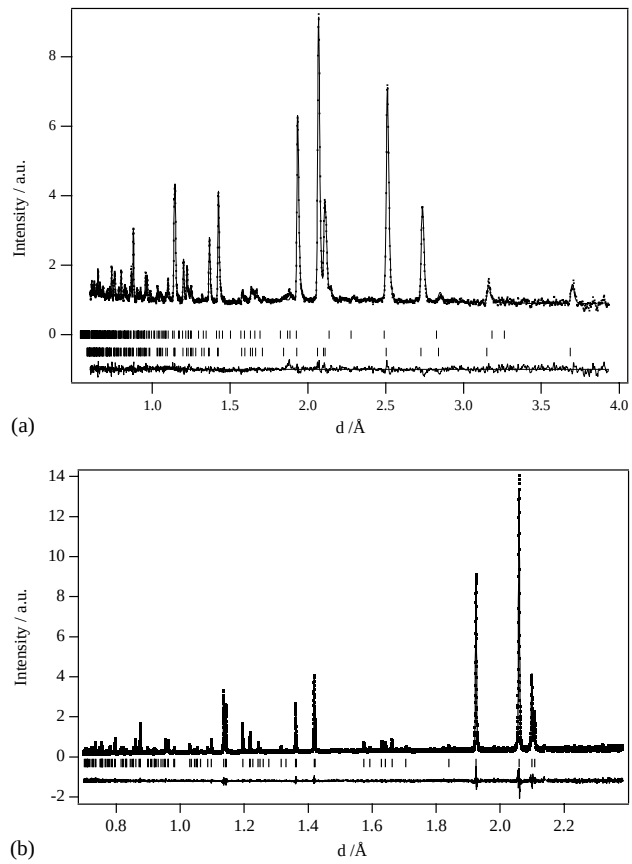

FIG. 2. Observed (■), calculated (—) and difference profiles of: (a) $La_2Sr_2ZnMnO_8$ (GEM 90° detector bank); the lower set of tick-marks indicate reflections from the main phase; the upper set represent reflections from the $La(OH)_3$ second phase. (b) $La_2Sr_2MgMnO_8$ (HRPD).

TABLE 1

Refined Atomic Coordinates for $La_2Sr_2MnZnO_8$ and $La_2Sr_2MnMgO_8$. Atomic Positions: La/Sr, *4e*, (0, 0, *z*); (Mg/Zn),/Mn, *2a*, (0, 0, 0), O1, *4e*, (0, 0, *z*); O2, *4c*, ($\frac{1}{2}$, 0, 0)

	$La_2Sr_2ZnMnO_8$	$La_2Sr_2MgMnO_8$
a (Å)	3.85503(3)	3.84863(1)
c (Å)	12.5960(2)	12.59344(6)
Volume (Å^3)	187.193(3)	186.534(1)
La/Sr		
z	0.36006(7)	0.35964(6)
U_{iso} (Å^2)	0.0052(2)	0.0111(4)
Mn/(Mg/Zn)		
U_{iso} Å^2	0.046(4)	0.027(3)
O_1		
z	0.16631(9)	0.16632(9)
U_{11} (Å^2)	0.0161(5)	0.0206(6)
U_{33} (Å^2)	0.0156(6)	0.0200(7)
O_2		
U_{11} (Å^2)	0.0052(6)	0.0114(7)
U_{22} (Å^2)	0.0081(6)	0.0127(8)
U_{33} (Å^2)	0.0081(6)	0.0140(8)
Bond lengths (Å)		
Mn,(Mg/Zn)-O_1 × 2	2.095(1)	2.094(1)
Mn,(Mg/Zn)-O_2 × 4	1.92752(1)	1.92432(1)
La,Sr–O_1 × 1	2.440(1)	2.435(2)
La,Sr–O_1 × 4	2.7461(2)	2.7409(2)
La,Sr–O_1 × 4	2.6120(5)	2.6129(5)

length scales probed by neutron powder diffraction should be visible. It can be seen that the data can be fitted well to a K_2NiF_4-like model in which Mn and Mg are disordered over the *B*-sites. Structural data derived from this refinement are tabulated in Table 1.

As was the case for $La_2Sr_2ZnMnO_8$, the atomic displacement parameter for the octahedrally coordinated Mn/Mg site is anomalously large, with the standard deviation being an order of magnitude greater than that of the other sites. This is again likely to reflect the opposed scattering lengths on that site, which reduce the mean scattering length to only 1.645(4) fm. The atomic displacement parameters for the other atoms are also relatively large, and we take this to indicate that significant static displacements occur in this structure as a consequence of the disorder on both the La/Sr and Mn/(Mg, Zn) sites.

3.2. Electron Diffraction

Figures. 3a and 3b present selected area diffraction patterns collected on $La_2Sr_2MgMnO_8$ in the [111] and [1$\bar{1}$0] projections, respectively. The patterns could not be indexed using the *I*4/*mmm* unit cell used in the neutron powder diffraction studies discussed above; rather a cell of dimensions $\sqrt{2}a \times \sqrt{2}a \times c$ was employed. It can be seen that the [111] pattern shows evidence for superstructure reflections with respect to the basic *I*4/*mmm* cell, and the [1$\bar{1}$0] pattern is similar to those for La_4LiMnO_8 and $La_3SrLiMnO_8$ (1), with $h\,h\,\xi$ rods of weak scattering being visible parallel to c*. These features are indicative of a structure with two-dimensional characteristics, that is ordering is present in the *xy* plane, but there is no repeat periodicity along *z*. These patterns suggest that the structural chemistry of $La_2Sr_2MgMnO_8$ is similar to that of La_4LiMnO_8 and $La_3SrLiMnO_8$ (1), with cation ordering within the *xy* perovskite sheets, these sheets being stacked in a disordered manner in *z*.

Figure 3c presents a selected area electron diffraction pattern from the [1$\bar{1}$0] zone axis of $La_2Sr_2ZnMnO_8$. It can be seen that very weak areas of intensity are present, halfway between the main reflections within experimental error ($\pm$0.5% in $1/d$), indicated as I and II. These weak features appear to be either diffuse, somewhat modulated rods, or Bragg reflections indicative of a large superstructure in *z*. Given the extremely weak intensity, it is not possible to determine unambiguously which of these possible interpretations is correct. The weakness of the features suggests that the difference in contrast is due to real-space ordering of Mn^{4+} and Zn^{2+}. If this is the case, an interpretation of

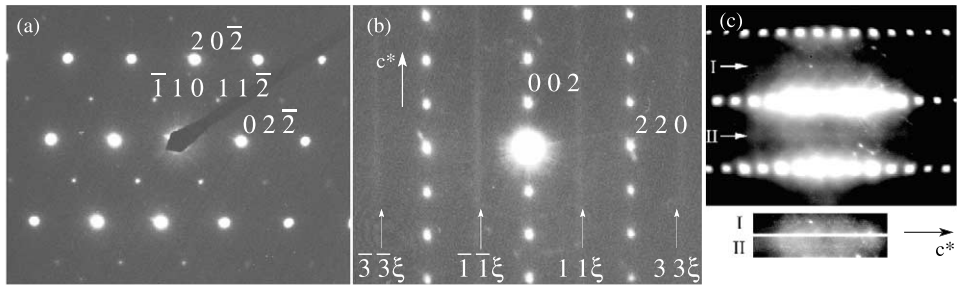

FIG. 3. (a) [111] and (b) [1$\bar{1}$0] zone axis SAED patterns of $La_2Sr_2MgMnO_8$. Both cells are indexed using a $\sqrt{2}a \times \sqrt{2}a \times c$ unit cell. (c) [1$\bar{1}$0] zone axis SAED pattern of $La_2Sr_2ZnMnO_8$. I and II are the rods referred to in the text.

these data in terms of cation ordering in xy, with disordered stacking of these xy layers in z is reasonable. Whether the possible modulation of the rods is intrinsic to the crystal, or simply due to a combination of statistical disordering in z and the limited area of the crystal studied is unclear. Given the highly similar electron scattering factors of Zn^{2+} and Mn^{4+}, it is unlikely that a high-resolution microscopy study would shed light on this matter.

3.3. Magnetization Measurements

Molar magnetic susceptibilities for $La_2Sr_2MgMnO_8$ and $La_2Sr_2ZnMnO_8$ are presented in Figs. 4a and 4b, respectively. It can be seen that both phases are best described as paramagnets in the temperature range $50 \leq T(K) \leq 300$. Below this temperature, the susceptibilities cannot be described using the Curie–Weiss law, even with the inclusion of a temperature-independent term. Fits to the Curie–Weiss law yielded negative Weiss constants (−39.1(8) and −64.3(8) K, respectively, for $La_2Sr_2MgMnO_8$ and $La_2Sr_2ZnMnO_8$), indicative of anti-ferromagnetic exchange interactions between Mn ions. This is in accord with the proposed exchange model for a B-site ordered material (1). The Curie constants derived from the fits are 1.934(5) and 1.875(9) emu mol^{-1} K^{-1}, respectively, which can be compared with the spin-only value for Mn^{4+} of 1.875 emu mol^{-1} K^{-1}. Attempts to fit the susceptibilities to a quadratic layer Heisenberg model (19) were not successful.

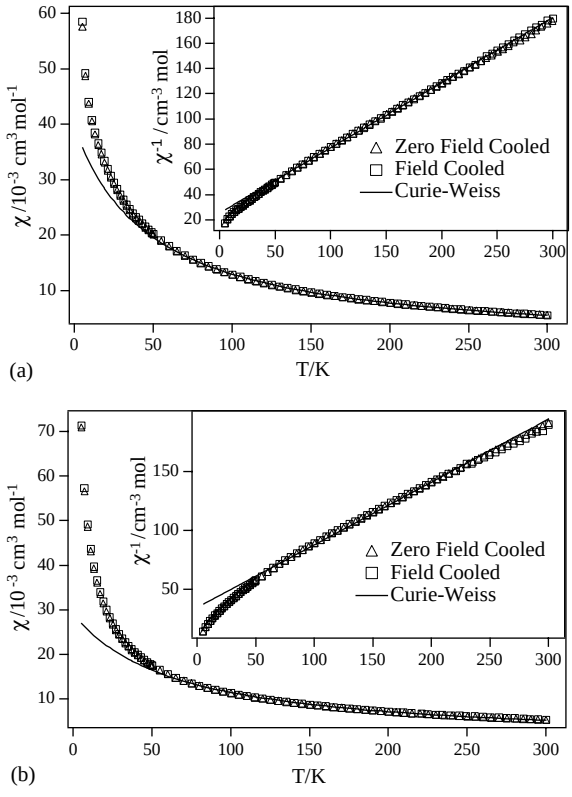

FIG. 4. Zero-field-cooled and field-cooled susceptibility (100 Oe) for (a) $La_2Sr_2MgMnO_8$ and (b) $La_2Sr_2ZnMnO_8$.

4. DISCUSSION

The structures of both of the compounds presented are best described on the X-ray and neutron diffraction length scale as tetragonal, $I4/mmm$, with a statistical (random) distribution of Mg/Zn and Mn over the six coordinate sites, using a K_2NiF_4-like unit cell. This is in contrast to the findings of Byeon *et al.* (14). Simulations were performed using the reported structure, and those of the disordered $I4/mmm$ cell. No difference was apparent between the two simulations, and we thus conclude that X-ray powder diffraction is insensitive to ordering of the type reported by Byeon, and that the space group $I4/mmm$ is a suitable description of the X-ray powder diffraction data. We note the contrast to La_4LiMnO_8 and $La_3SrLiMnO_8$ (1), which could be thus described on the length scale of an X-ray powder diffraction experiment, but on the length scale probed by a neutron diffraction experiment were best considered as possessing expanded unit cells of dimensions $\sqrt{2}a \times \sqrt{2}b \times c$, where a, b and c here refer to the tetragonal K_2NiF_4-like cell, albeit with strong disordering along c. This ordering was apparent when the Mn sites were 'labelled' with an ordered spin; without this spin 'label' the similarity in scattering lengths of Li and Mn prevented the two sites being distinguished. Given the large difference in neutron scattering lengths of Mg/Zn and Mn, if $La_2Sr_2MgMnO_8$ and $La_2Sr_2ZnMnO_8$ possess similar structures to those of La_4LiMnO_8 and $La_3SrLiMnO_8$, we would expect to see evidence for long-range cation ordering in the room temperature neutron powder diffraction patterns. That scattering due to such long-range ordering is not apparent is taken to indicate that the cation ordering occurs over far smaller xy regions in the Zn and Mg substituted materials than in the Li analogs, below the length scales probed by neutron powder diffraction.

Evidence of ordering in xy, albeit with similar structural paracrystallinity to that observed in the Li-analog, is provided by the electron diffraction experiments described above, and thus it would appear that the xy cation ordering in $La_2Sr_2MgMnO_8$ and $La_2Sr_2ZnMnO_8$ occurs on a length scale lower than that of a neutron diffraction experiment, but greater than that an electron diffraction experiment. This suggests that $2D$, chessboard-ordered clusters exist over a small xy length scale, and are broken up either by disordered regions, or by linear defects.

The magnetic behavior of $La_2Sr_2MgMnO_8$ and $La_2Sr_2ZnMnO_8$ likewise contrasts with that of La_4LiMnO_8 and $La_3SrLiMnO_8$. For the Li-containing phases, magnetic ordering was apparent from the susceptibility

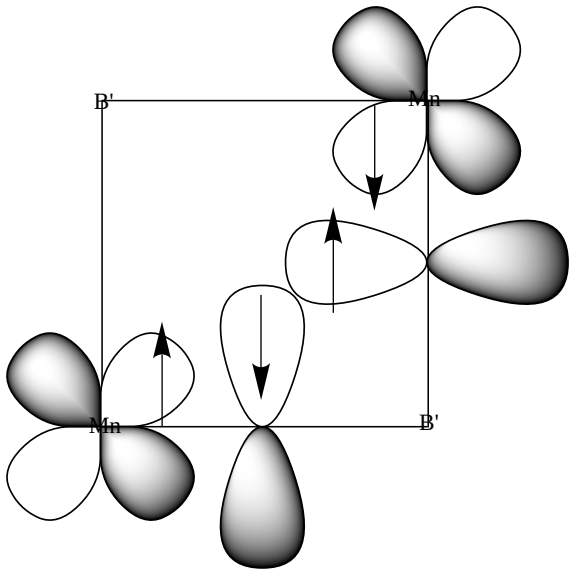

FIG. 5. Schematic representation of the π superexchange pathway in the xy plane of the K_2NiF_4 structure with cation ordering over the octahedral sites.

measurements around 20 K, whereas for the Mg and Zn materials, there was no clear evidence for a magnetic transition in the temperature range $5 \leq T(\mathrm{K}) \leq 300$. A possible explanation for this behavior is that the presence of the relatively electronegative Mg^{2+} or Zn^{2+} on the site B′ (Fig. 5) causes a greater withdrawal of electron density from the bridging O^{2-} $p\pi$ orbitals leading to a weakening in the Mn–O–O–Mn coupling between the Mn^{4+} centres. This is in contrast with the Li-containing analogues, in which interactions between next-nearest neighbor sites (Mn–Mn) were significant. Furthermore, the lack of long-range xy cation ordering, as suggested by the neutron diffraction experiments, is expected to oppose the formation of a long-range ordered magnetic ground state. Given the bond percolation threshold of 50% for a square lattice (20), it is unlikely that long-range magnetic ordering will be favored, especially as, in the absence of strong next-nearest-neighbor interactions, the presence of short-range cation ordering is expected to raise this threshold significantly.

5. CONCLUSION

The structural and magnetic chemistry of $La_2Sr_2MgMnO_8$ and $La_2Sr_2ZnMnO_8$ provides a contrast to that of isoelectronic $La_3SrLiMnO_8$. Substitution of Li^+ with the divalent Mg^{2+} or Zn^{2+}, while changing the La/Sr ratio to preserve the Mn^{4+} charge, has had the effect of greatly reducing the inter-Mn coupling constant J. This is thought to be a result of the increased electronegativity of Mg^{2+} and Zn^{2+} with respect to that of Li^+, causing a decrease in electron density at the bridging $p\pi$ oxide ions. Further, the electron diffraction data indicate that complete xy cation chessboard-type ordering occurs locally, with the chessboard layers stacked randomly along z. This xy ordering does not persist over the length scale probed through neutron or X-ray diffraction, and thus the formation of finite sized areas, ordered in xy, seems likely. This is expected to suppress the formation of long-range magnetic order on cooling.

Although both $La_2Sr_2MgMnO_8$ and $La_2Sr_2ZnMnO_8$ possess structures which are different to those of the Li-containing phases, the structures of these materials are not as simple as X-ray and neutron diffraction might suggest. From these studies, it appears likely that the structures of a number of K_2NiF_4-like materials which appear disordered over the X-ray and neutron length scale, perhaps including phases related to the superconducting $La_{2-x}Sr_xCuO_4$, are actually ordered over the length scales relevant in the study of electronic properties. This suggests that caution should be used in interpreting the electronic structure and chemistry of K_2NiF_4-like materials in terms of the diffraction-averaged structures observed.

ACKNOWLEDGMENTS

We thank R. M. Ibberson and P. G. Radaelli for experimental assistance at ISIS, and to acknowledge the EPSRC for support.

REFERENCES

1. J. C. Burley, P. D. Battle, D. J. Gallon, J. Sloan, C. P. Grey, and M. J. Rosseinsky, *J. Am. Chem. Soc.* **124,** 620 (2002).
2. S. K. Yeh, S. Y. Wu, and Y. Wang, *Acta Crystallogr. B* **49,** 806 (1993).
3. R. Hosemann, *Z. Phys.* **128,** 465 (1950).
4. A. M. Hindeleh and R. Hosemann, *J. Phys. C* **21,** 4155 (1988).
5. G. Demazeau, E. O. Okhim, K. T. Wang, L. Fournes, J. M. Dance, M. Pouchard, and P. Hagenmüller, *Rev. de Chim. Miner.* **24,** 183 (1987).
6. S. H. Byeon, G. Demazeau, L. Fournes, J. M. Dance, and J. H. Choy, *Solid State Commun.* **80,** 457 (1991).
7. J. P. Attfield and G. Ferey, *J. Solid State Chem.* **80,** 112 (1989).
8. G. Demazeau, M. Pouchard, L. M. Zhu, and P. Hagenmüller, *Z. Anorg. Allg. Chem.* **555,** 64 (1987).
9. G. Villeneuve, T. Rojo, G. Demazeau, and P. Hagenmüller, *Mater. Res. Bull.* **23,** 1787 (1988).
10. Z. Li-Ming, G. Demazeau, L. Fournes, M. Pouchard, and P. Hagenmüller, *C. R. Acad. Sci. (Paris)* **304,** 633 (1987).
11. W. Pietzuch, S. A. Warda, W. Massa, and D. Reinen, *Z. Anorg. Allg. Chem.* **626,** 113 (2000).
12. S. A. Warda, W. Massa, D. Reinen, Z. W. Hu, G. Kaindl, and F. M. F. deGroot, *J. Solid State Chem.* **146,** 79 (1999).
13. S. Abou-Warda, W. Pietzuch, G. Berghofer, U. Kesper, W. Massa, and D. Reinen, *J. Solid State Chem.* **138,** 18 (1998).
14. S. H. Byeon, I. S. Kim, M. Itoh, and T. Nakamura, *Mater. Res. Bull.* **28,** 597 (1993).

15. H. M. Rietveld, *Acta Crystallogr*. **22,** 151 (1967).
16. H. M. Rietveld, *J. Appl. Crystallogr*. **2,** 65 (1969).
17. A. C. Larson and R. B. Von Dreele, General Structure Analysis System (GSAS), Technical Report LAUR 86-748, Los Alamos National Laboratory, 1990.
18. V. F. Sears, *Neutron News* **3,** 26 (1992).
19. M. E. Lines, *J. Phys. Chem. Solids* **31,** 101 (1970).
20. J.A. Mydosh, ''Spin Glasses—An Experimental Introduction.'' Taylor & Francis, London, 1993.